Test Bench - Nano-Hexapod Struts

Dehaeze Thomas

March 27, 2024

Contents

In this document, a test-bench is used to characterize the struts of the nano-hexapod.

Each strut includes (Figure 1):

- 2 flexible joints at each ends. These flexible joints have been characterized in a separate test bench (see ...).
- 1 Amplified Piezoelectric Actuator (APA300ML) (described in Section ...). Two stacks are used as an actuator and one stack as a (force) sensor.
- 1 encoder (Renishaw Vionic) that has been characterized in a separate test bench (see ...).

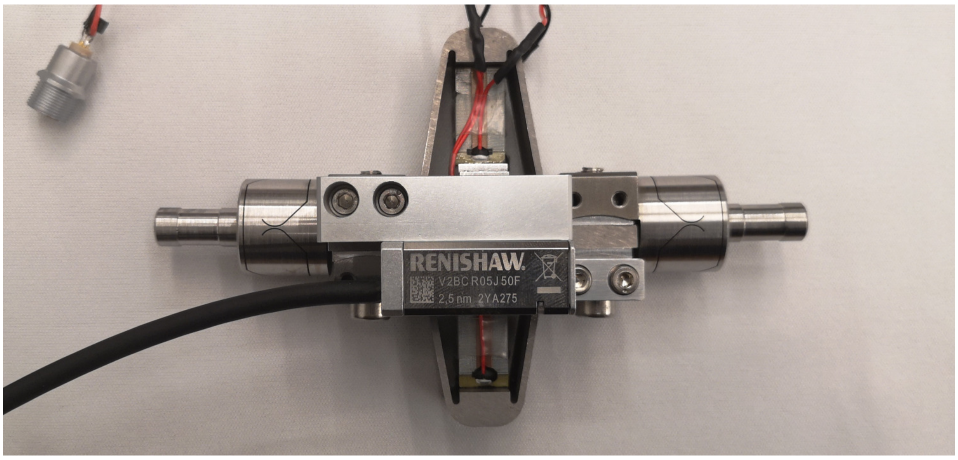

Figure 1: One strut including two flexible joints, an amplified piezoelectric actuator and an encoder

Then the struts are mounted (procedure described in Section 1), and are fixed to the same measurement bench. The goals are to:

- Section 3: Identify the dynamics from the generated DAC voltage to:
  - the sensors stack generated voltage
  - the measured displacement by the encoder
  - the measured displacement by the interferometer (representing encoders that would be fixed to the nano-hexapod's plates instead of the struts)
- Section 4: Compare the measurements with the Simscape model of the struts and tune the models

The final goal of the work presented in this document is to have an accurate Simscape model of the struts that can then be included in the Simscape model of the nano-hexapod.

Table 1: Report sections and corresponding Matlab files

Sections	**Matlab File**
Section 2	`test_struts_1_flexible_modes.m`
Section 3	`test_struts_2_dynamical_meas.m`
Section 4	`test_struts_3_simscape_model.m`

1 Mounting Procedure

1.1 Mounting Bench

A mounting bench is used to greatly simply the mounting of the struts as well as ensuring the correct strut length and coaxiality of the flexible joint's interfaces. This is very important in order to not loose any stroke when the struts will be mounted on the nano-hexapod.

A CAD view of the mounting bench is shown in Figure 1.1.

Faro arm[1]

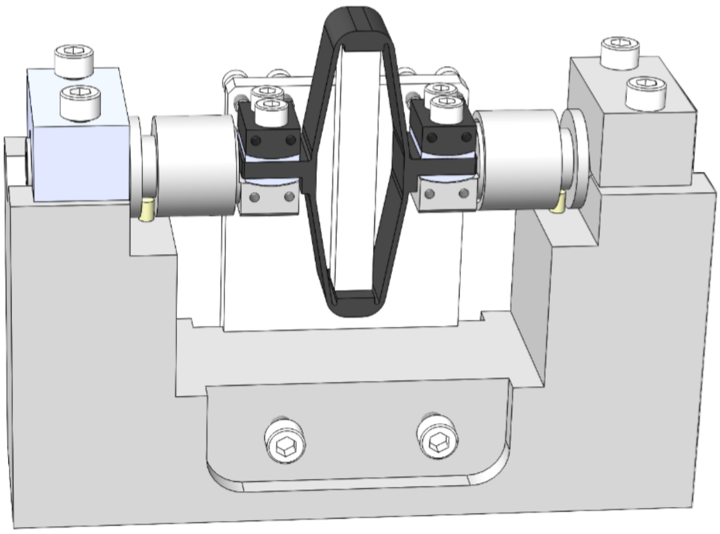

Figure 1.1: CAD view of the mounting bench

The main part of the bench is here to ensure both the correct strut length and strut coaxiality as shown in Figure 1.2a.

The tight tolerances of this element has been verified as shown in Figure 1.2b and were found to comply with the requirements.

The flexible joints are rigidly fixed to cylindrical tools shown in Figures 1.3a and 1.3b which are then mounted on the mounting tool shown in Figure 1.2a. This cylindrical tool is here to protect the flexible joints when tightening the screws and therefore applying large torque.

[1] Faro Arm Platinum 4ft, specified accuracy of $\pm 13 \mu m$

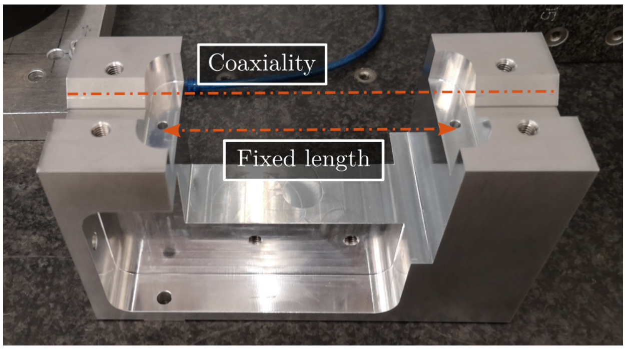

(a) Useful features of the main mounting element

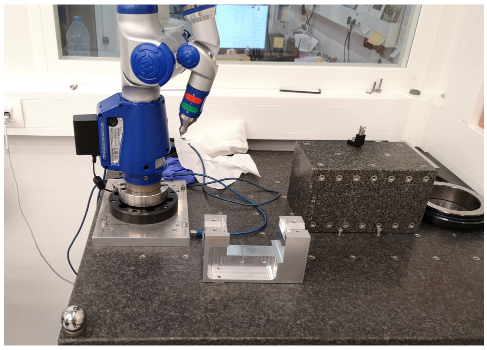

(b) Dimensional check

Figure 1.2: Caption…, add foot note with Faro arm

1.2 Mounting Procedure

Better explain the mounting procedure

Speak about the “locating” pins that are used to aligned the APA with the two flexible joints

The mounting procedure is as follows:

1. Screw flexible joints inside the cylindrical interface element shown in Figure 1.3
2. Fix the two interface elements. One of the two should be clamped, the other one should have its axial rotation free. Visually align the clamped one horizontally. (Figure 1.4a)
3. Put cylindrical washers, APA and interface pieces on top of the flexible joints (Figure 1.4b)
4. Put the 4 screws just in contact such that everything is correctly positioned and such that the “free” flexible joint is correctly oriented
5. Put the 8 lateral screws in contact
6. Tighten the 4 screws to fix the APA on the two flexible joints (using a torque screwdriver)
7. Remove the 4 laterals screws
8. (optional) Put the APA horizontally and fix the encoder and align it to maximize the contrast (Figure 1.4c)
9. Disassemble to have an properly mounted strut (Figure 1.4d) for which the coaxiality between the two flexible joint’s interfaces is good

(a) Cylindral Interface (Top) **(b)** Cylindrlcal Interface (Bottom) **(c)** Mounted flexible joints

Figure 1.3: Preparation of the flexible joints by fixing them in their cylindrical interface

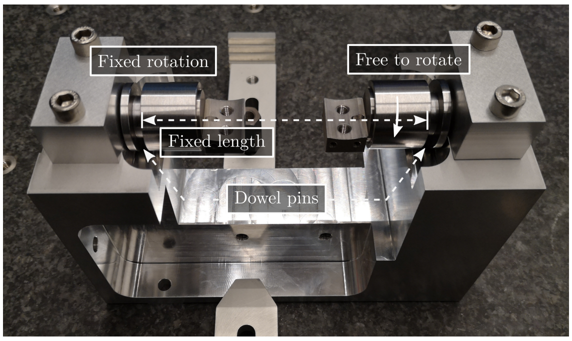

(a) Step 1

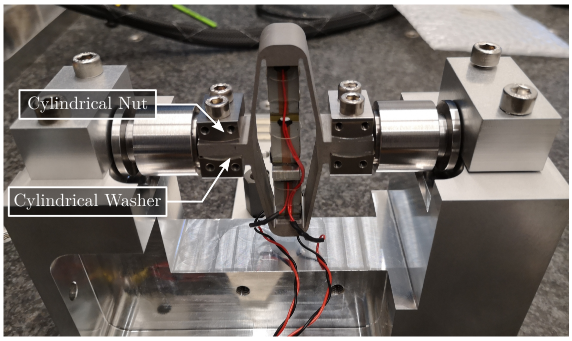

(b) Step 2

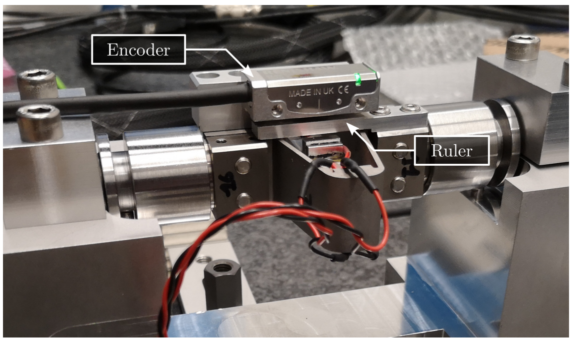

(c) Step 3

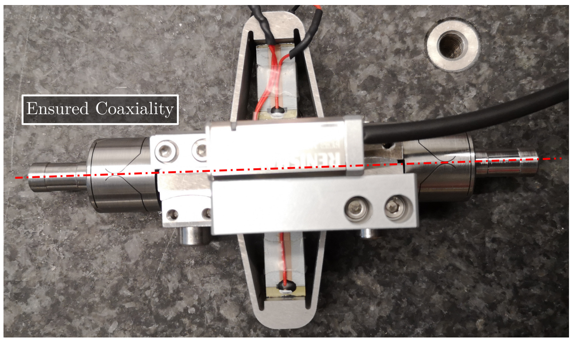

(d) Step 4

Figure 1.4: Steps for mounting the struts.

2 Measurement of flexible modes

2.1 Introduction

From a Finite Element Model of the struts, it have been found that three main resonances are foreseen to be problematic for the control of the APA300ML (Figure 2.1): an "X-bending" mode at 189Hz, a "Y-bending" mode at 285Hz and a "Z-torsion" mode at 400Hz.

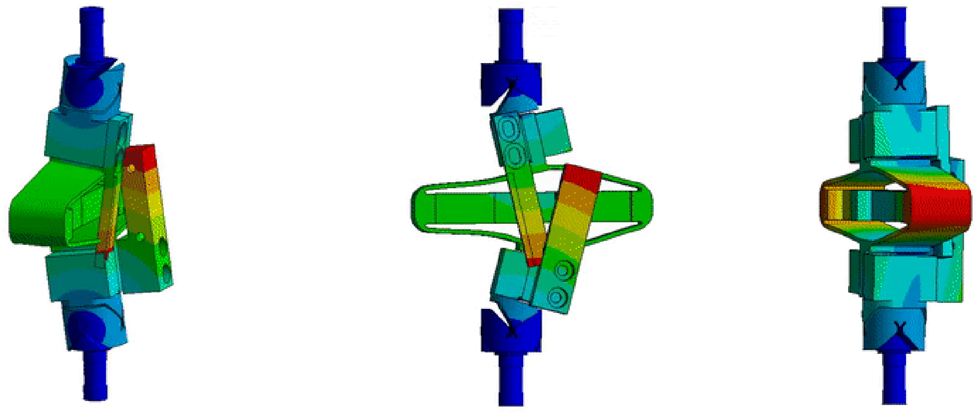

(a) X-bending mode (189Hz) **(b)** Y-bending mode (285Hz) **(c)** Z-torsion mode (400Hz)

Figure 2.1: Spurious resonances of the struts estimated from a Finite Element Model

2.2 Measurement Setup

A Laser vibrometer is measuring the difference of motion between two beam path (red points in Figure 2.2). The strut is excited with an instrumented hammer and the transfer function from the hammer to the measured rotation is computed.

The "X-bending" mode is measured as shown in Figure 2.2a. The "Y-bending" mode is measured as shown in Figure 2.2b. Finally, the "Z-torsion" is measured as shown in Figure 2.2c.

This is done with and without the encoder fixed to the strut.

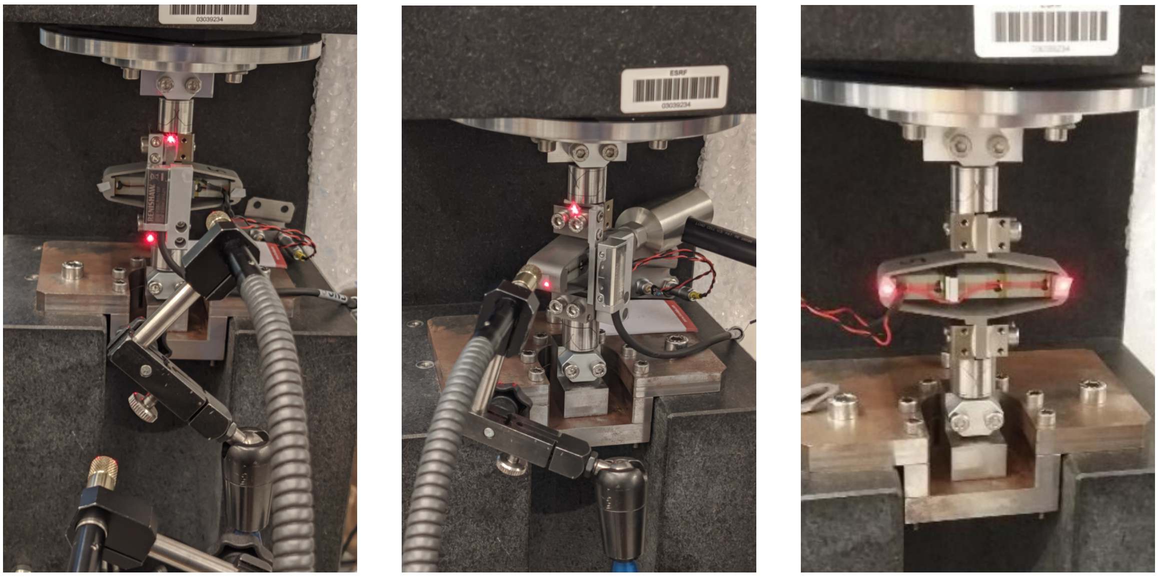

(a) X-bending mode **(b)** Y-bending mode **(c)** Z-torsion mode

Figure 2.2: Measurement of strut flexible modes

2.3 Measured results

The obtained frequency response functions are shown in Figure 2.3.

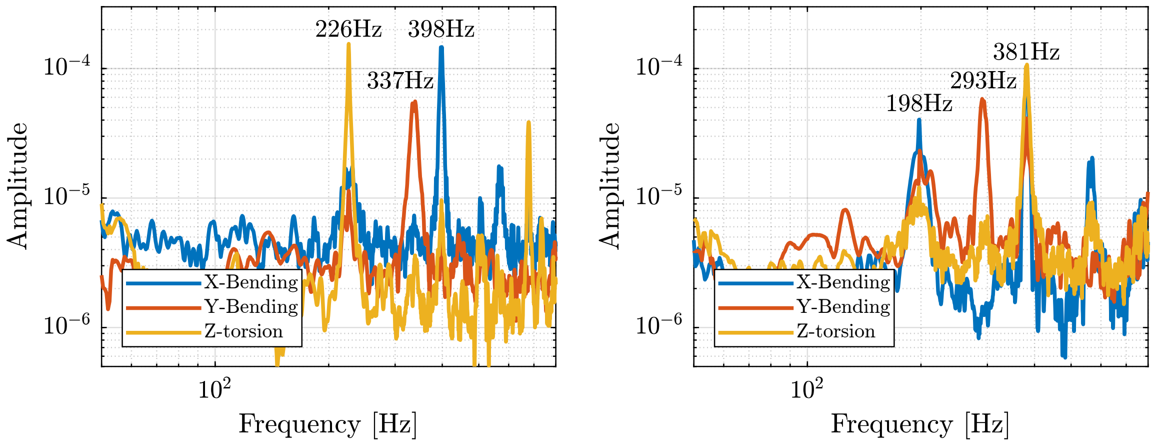

(a) without encoder **(b)** with the encoder

Figure 2.3: Measured frequency response functions without the encoder 2.3 and with the encoder 2.3b

Table 2.1 summarizes the measured resonance frequencies as well as the computed ones using the Finite Element Model. It is shown that:

- the resonance frequencies of the 3 modes are only slightly increasing when the encoder is removed
- the computed resonance frequencies from the FEM are very close to the measured one when the

encoder is fixed to the strut

Table 2.1: Measured frequency of the strut spurious modes

Mode	Struts (FEM)	Struts (exp)	Plates (exp)
X-Bending	189Hz	198Hz	226Hz
Y-Bending	285Hz	293Hz	337Hz
Z-Torsion	400Hz	381Hz	398Hz

3 Dynamical measurements

The bench is shown in Figure 3.1a. Measurements are performed either when no encoder is fixed to the strut (Figure 3.1b) or when one encoder is fixed to the strut (Figure 3.1c).

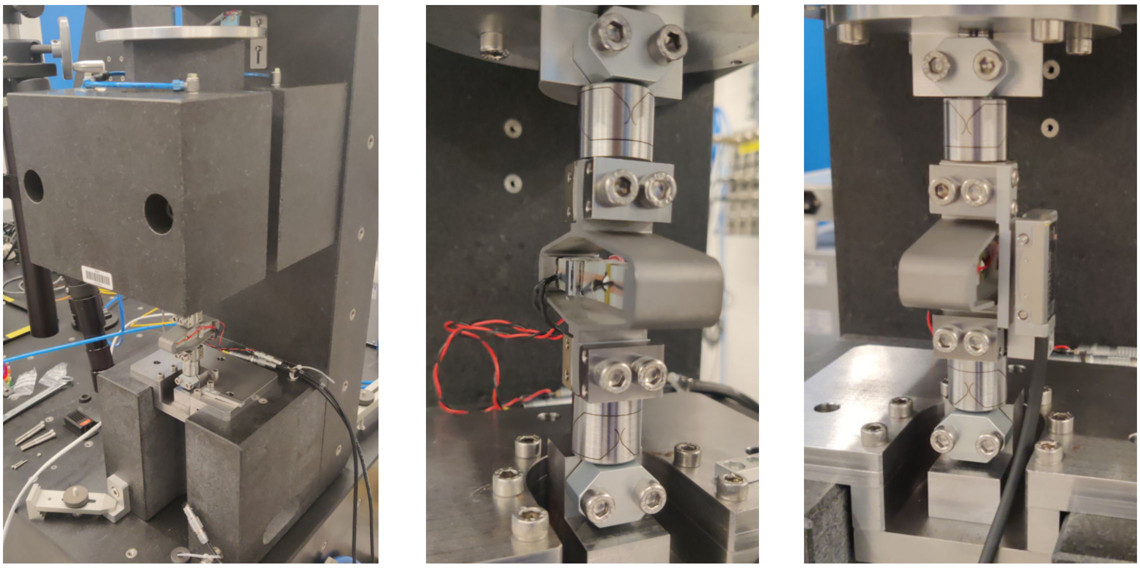

(a) Overview **(b)** Strut without encoder **(c)** Strut with encoder

Figure 3.1: Experimental setup to measured the dynamics of the struts.

First, the effect of the encoder on the measured dynamics is studied in Section 3.1. Then, the dynamics seen by the encoder and by the interferometers are compared in Section 3.2. Finally, all the measured struts are compared in terms of dynamics in Section 3.3.

3.1 Effect of the Encoder on the measured dynamics

Figure 3.2a Same goes for the transfer function from excitation voltage u to the axial motion of the strut d_a as measured by the interferometer ().

The transfer function from the excitation voltage u to the generated voltage V_s by the sensor stack is not influence by the fixation of the encoder (Figure 3.2b). This means that the IFF control strategy should be as effective whether or not the encoders are fixed to the struts.

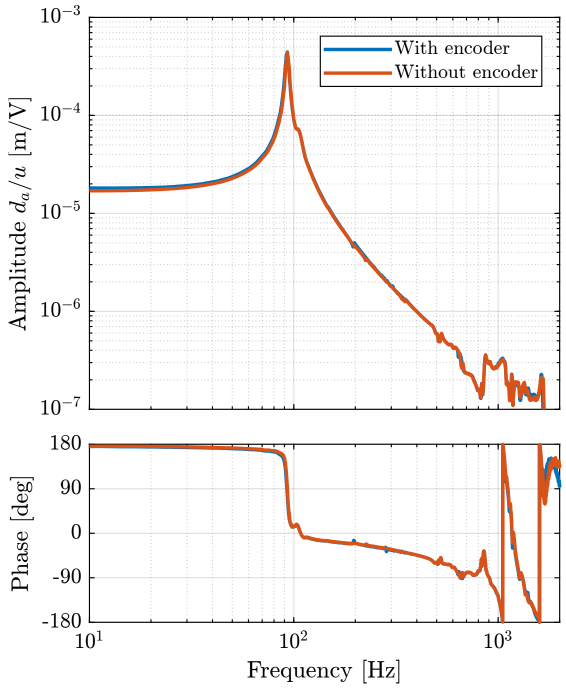

(a) u to d_a

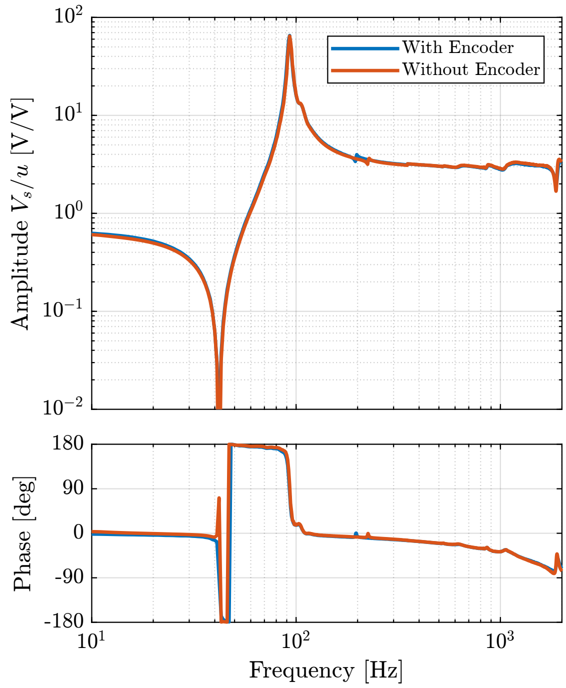

(b) u to V_s

Figure 3.2: Effect of having the encoder fixed to the struts on the measured dynamics from u to d_a (a) and from u to V_s (b)

3.2 Comparison of the encoder and interferometer

The dynamics as measured by the encoder and by the interferometers are compared in Figure 3.3.

The dynamics from the excitation voltage u to the measured displacement by the encoder d_e presents much more complicated behavior than the transfer function to the displacement as measured by the Interferometer (compared in Figure 3.3). It will be further investigated why the two dynamics as so different and what are causing all these resonances.

As shown in Figure 3.3, we can clearly see three spurious resonances at 197Hz, 290Hz and 376Hz. These resonances correspond to parasitic resonances of the strut itself that was estimated using a finite element model of the strut (Figure 2.1):

- Mode in X-bending at 189Hz
- Mode in Y-bending at 285Hz
- Mode in Z-torsion at 400Hz

The good news is that these resonances are not seen on the interferometer (they are therefore not impacting the axial motion of the strut). But these resonances are making the use of encoder fixed to the strut difficult.

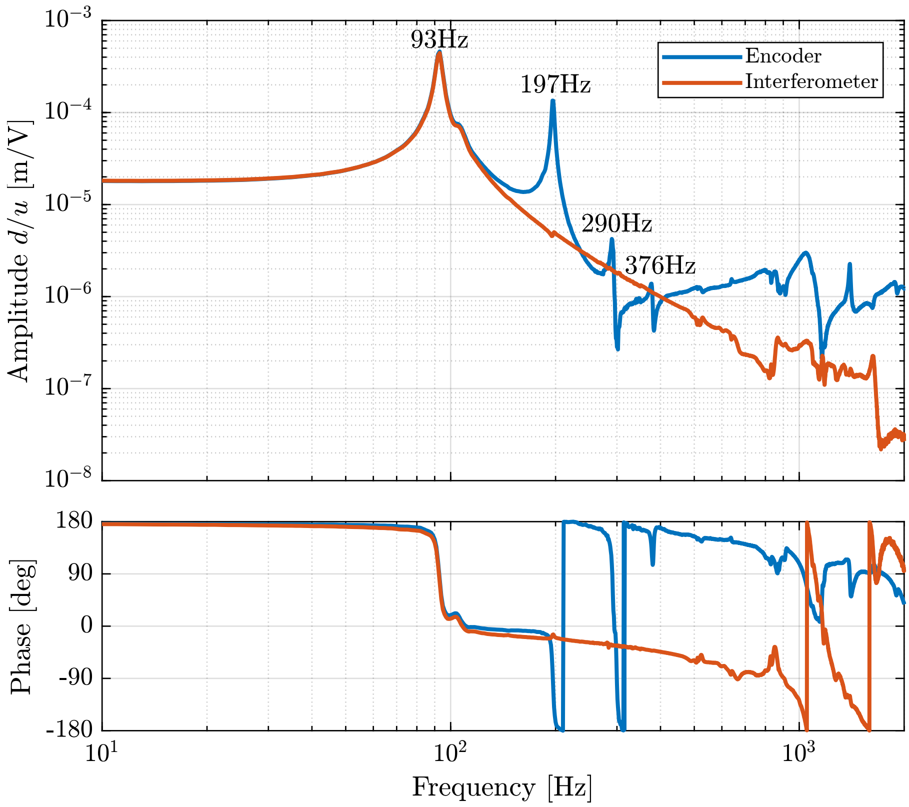

Figure 3.3: Comparison of the transfer functions from excitation voltage u to either the encoder d_e or the interferometer d_a

3.3 Comparison of all the Struts

Then, the transfer function from the DAC output voltage u to the measured displacement by the Attocube is computed for all the struts and shown in Figure 3.4a. All the struts are giving very similar FRF.

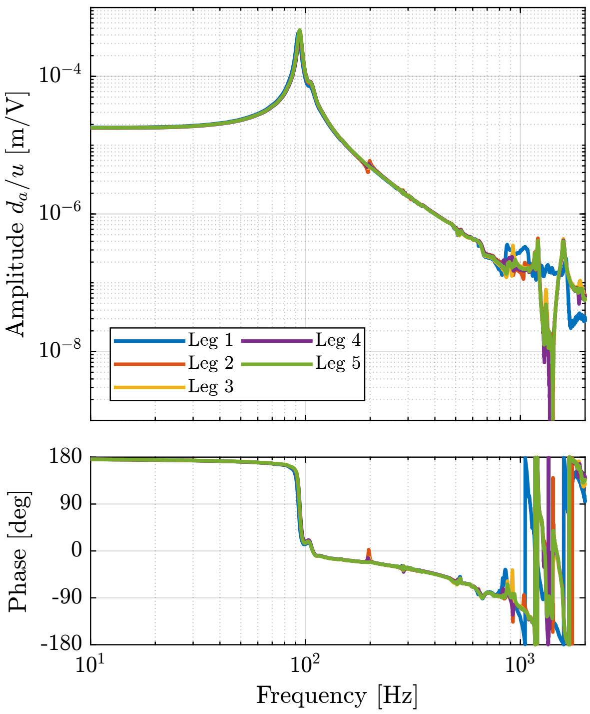

(a) u to d_a

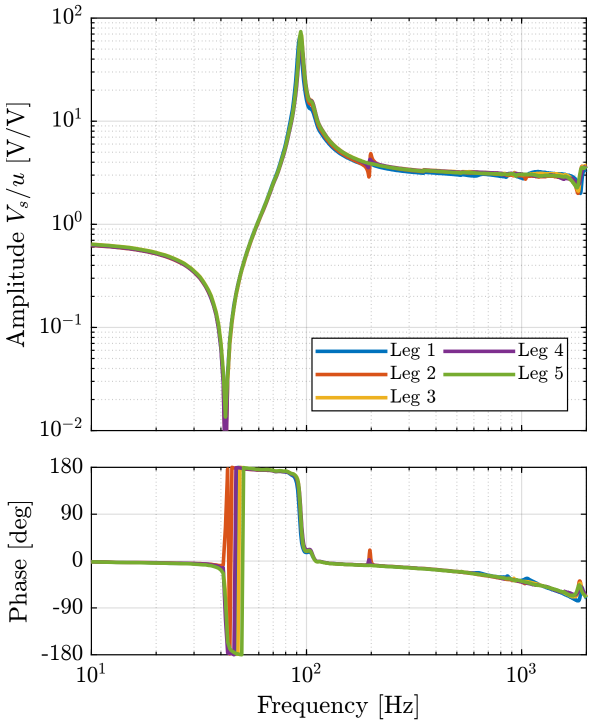

(b) u to V_s

Figure 3.4: Comparison of the measured plants

There is a very large variability of the dynamics as measured by the encoder as shown in Figure 3.5. Even-though the same peaks are seen for all of the struts (95Hz, 200Hz, 300Hz, 400Hz), the amplitude of the peaks are not the same. Moreover, the location or even the presence of complex conjugate zeros is changing from one strut to the other.

All of this will be studied in Section 4 using the Simscape model.

Important

All the struts are giving very consistent behavior from the excitation voltage u to the force sensor generated voltage V_s and to the interferometer measured displacement d_a. However, the dynamics from u to the encoder measurement d_e is much more complex and variable from one strut to the other most likely due to poor alignment of the APA with respect to the flexible joints.

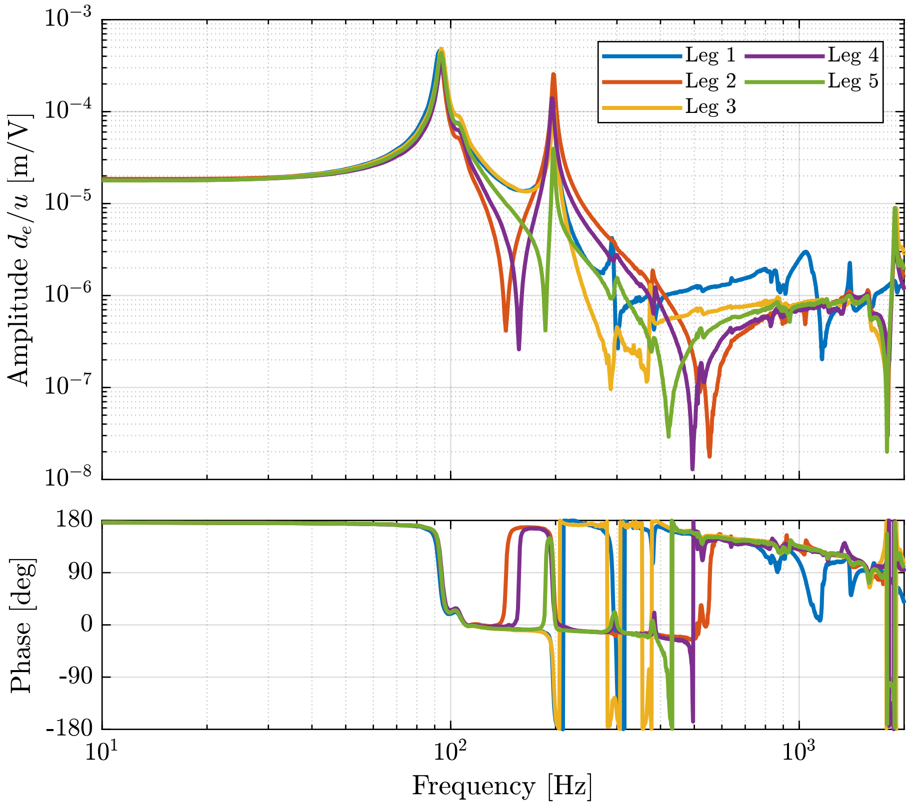

Figure 3.5: Estimated frequency response functions from u to the encoder d_e for all the mounted struts

4 Simscape Model

However, now the full strut is put instead of only the APA (see Figure 4.1).

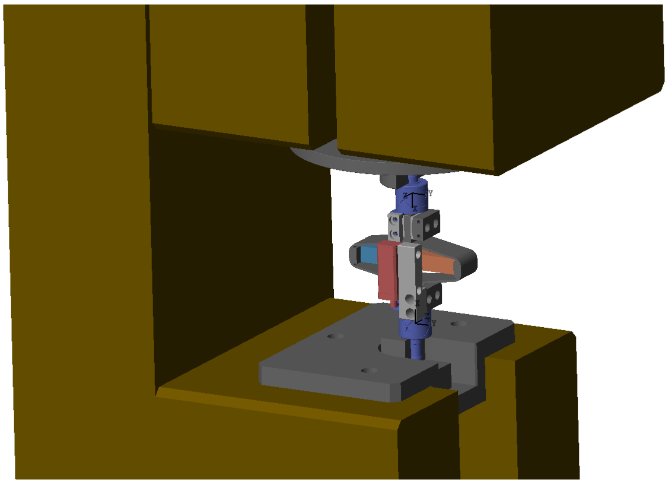

Figure 4.1: Screenshot of the Simscape model of the strut fixed to the bench

This Simscape model is used to:

- compare the measured FRF with the modelled FRF
- help the correct understanding/interpretation of the results
- tune the model of the struts (APA, flexible joints, encoder)

This study is structured as follow:

- Section 4.1: the measured FRF are compared with the Simscape model.
- Section 4.2: the flexible APA model is used, and the effect of a misalignment of the APA and flexible joints is studied. It is found that the misalignment has a large impact on the dynamics from u to d_e.
- Section 4.5: the effect of the flexible joint's stiffness on the dynamics is studied. It is found that the axial stiffness of the joints has a large impact on the location of the zeros on the transfer function from V_s to d_e.

4.1 Model dynamics

Two models of the APA300ML are used here for comparison:

- a simple two degrees of freedom model
- a model using a super element extracted from a finite element model

These two models of the APA300ML were tuned to best match measured frequency response functions of the APA alone. The flexible joints are here modelled with the 4DoF model (axial stiffness, two bending stiffnesses and one torsion stiffness).

These two models are compared with the measured frequency responses in Figure 4.2.

The model dynamics from DAC voltage u to the axial motion of the strut d_a (Figure 4.2a) and from DAC voltage u to the force sensor voltage V_s (Figure 4.2c) are well matching the experimental identification.

However, the transfer function from u to encoder displacement d_e are not well matching for both models. For the 2DoF model, this is normal as the resonances affecting the dynamics are not modelled at all (the APA300ML is modelled as infinitely rigid in all directions except the translation along it's actuation axis). For the flexible model, it will be shown in the next section that by adding some misalignment betwen the flexible joints and the APA300ML, this model can better represent the observed dynamics.

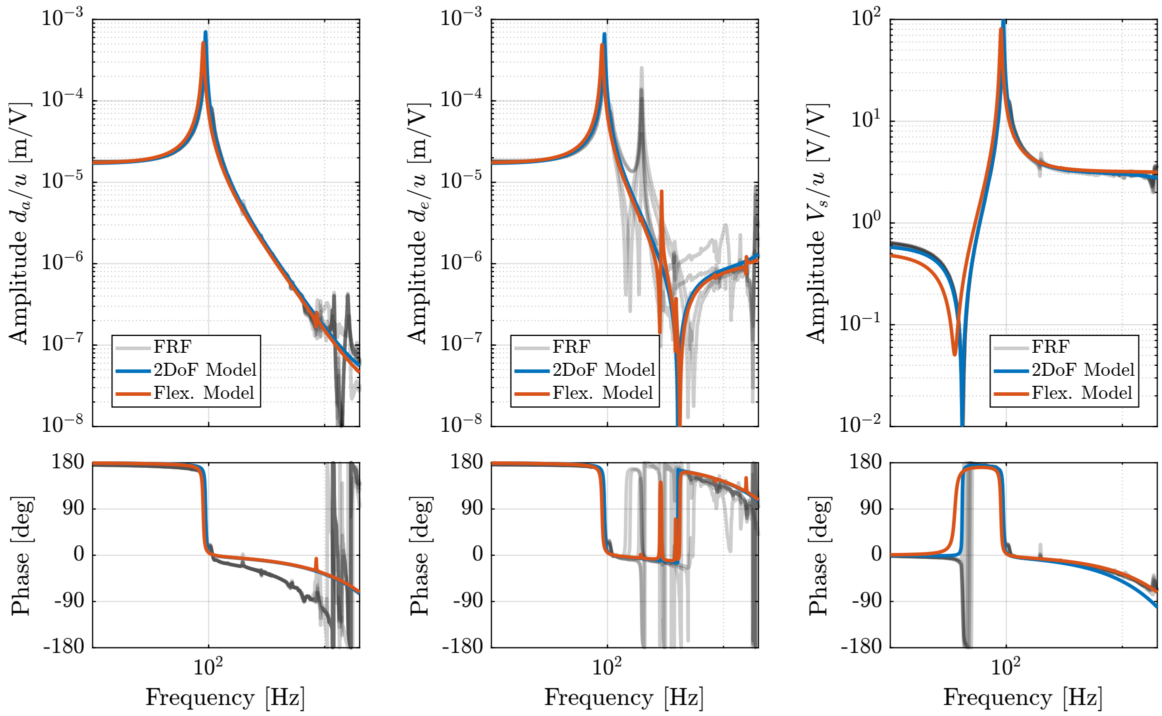

(a) u to d_a **(b)** u to d_e **(c)** u to V_s

Figure 4.2: Comparison of the measured dynamics and of the Simscape dynamics using the "flexible" APA300ML model (Super-Element extracted from a Finite Element Model).

4.2 Effect of strut misalignment

As was shown in Figure 3.5, the identified dynamics from DAC voltage u to encoder measured displacement d_e are very different from one strut to the other.

In this section, it is investigated whether poor alignment of the strut (flexible joints with respect to the APA) can explain such dynamics. For instance, consider Figure 4.3 where there is a misalignment in the y direction between the two flexible joints (well aligned thanks to the mounting procedure in Section 1) and the APA300ML. In such case, the "x-bending" mode at 200Hz (see Figure 2.2a) can be expected to be more excited, and thus the dynamics from the actuator to the encoder should be affected at frequencies around 200Hz.

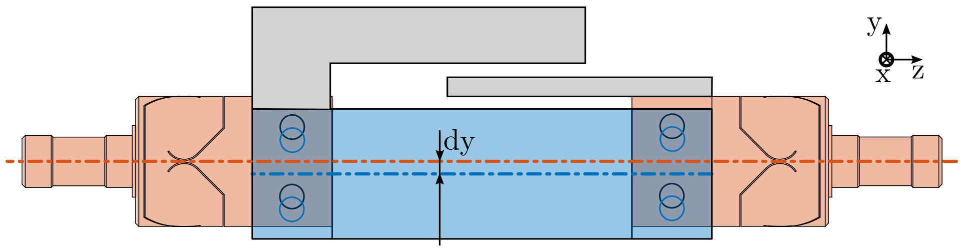

Figure 4.3: Mis-alignement between the joints and the APA

To verify this assumption, the dynamics from output DAC voltage u to the measured displacement by the encoder d_e is computed using the Simscape model with flexible APA for several misalignment in the y direction. Obtained dynamics are shown in Figure 4.4a. The alignment of the APA with the flexible joints as a **huge** influence on the dynamics from actuator voltage to measured displacement by the encoder. The misalignment in the y direction mostly influences:

- the presence of the flexible mode at 200Hz (see mode shape in Figure 2.1a)
- the location of the complex conjugate zero between the first two resonances:
  - if $d_y < 0$: there is no zero between the two resonances and possibly not even between the second and third ones
  - if $d_y > 0$: there is a complex conjugate zero between the first two resonances
- the location of the high frequency complex conjugate zeros at 500Hz (secondary effect, as the axial stiffness of the joint also has large effect on the position of this zero)

The same can be done for a misalignment in the x direction. The obtained dynamics are shown in Figure 4.4b where it is shown that misalignment in the x direction mostly influences the presence of the flexible mode at 300Hz (see mode shape in Figure 2.1b).

Comparing the experimental frequency response functions for all the APA in Figure 3.5 with the model dynamics for several y misalignments in Figure 4.4a indicates a clear similarity. This similarity suggests that the identified differences in dynamics are caused by the misalignment.

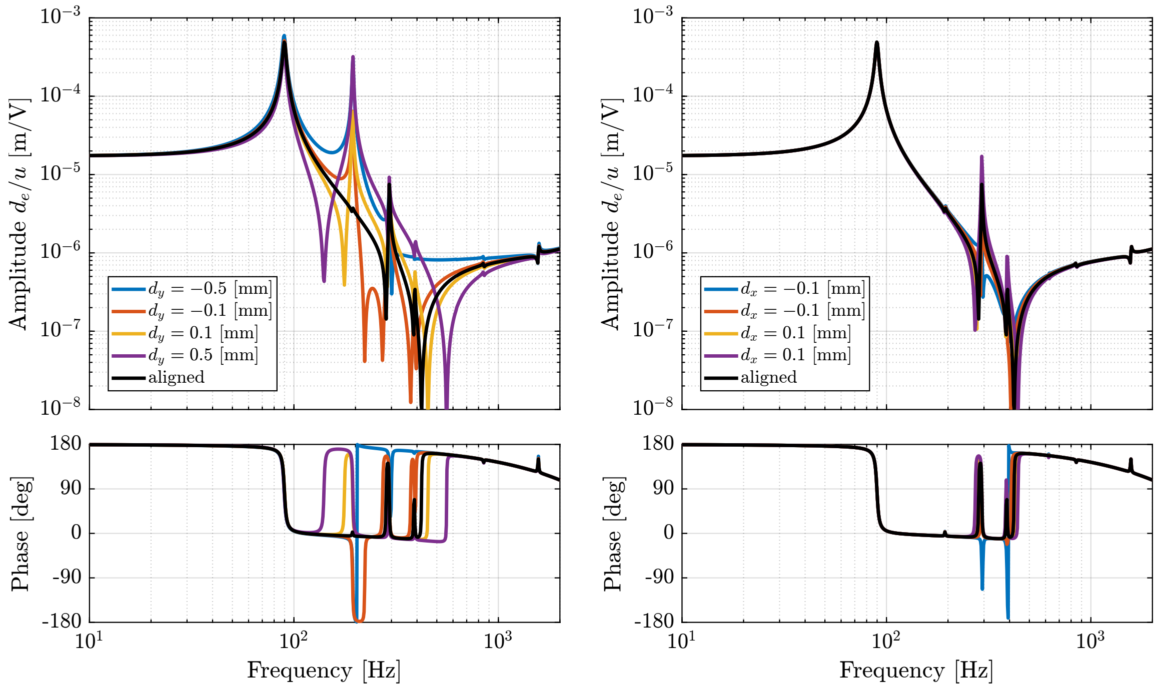

(a) Misalignment along y

(b) Misalignment along x

Figure 4.4: Effect of a misalignment between the flexible joints and the APA300ML in the y direction (a) and in the x direction (b)

4.3 Measured strut misalignment

During the first mounting of the struts presented in Section 1, the positioning pins used to position the APA with respect to the flexible joints in the y directions were not used (not received at the time). Therefore, large y misalignments may be expected.

In order to estimate the misalignments between the two flexible joints and the APA:

- the struts are fixed horizontally to the mounting bench as shown in Figure 1.4c but without the encoder
- using a length gauge[1], the height difference from the flexible joints surface and the APA shell surface is measured both for the top and bottom joints and on both sides
- as the thickness of the flexible joint is $21\,mm$ and the thickness of the APA shell is $20\,mm$, $0.5\,mm$ of height different should be measured is the two are perfectly aligned

Large variations in the y misalignment are found from one strut to the other (results are summarized in Table 4.1).

To check the validity of the measurement, it can be verified that sum of the measured thickness difference on each side is $1\,mm$ (equal to the thickness difference between the flexible joint and the APA). This thickness differences for all the struts were found to be between $0.94\,mm$ and $1.00\,mm$ which indicate low errors as compared to the misalignments found in Table 4.1.

Table 4.1: Measured y misalignment at the top and bottom of the APA. Measurements are in mm

Strut	Bot	Top
1	0.1	0.33
2	-0.19	0.14
3	0.41	0.32
4	-0.01	0.54
5	0.15	0.02

By using the measured y misalignment in the Simscape model with the flexible APA model, the measured dynamics from u to d_e can be approached as shown in Figure 4.5. Even better match in the dynamics can be obtained by fine tuning both the x and y misalignments (yellow curves in Figure 4.5).

This confirms that the misalignment between the APA and the strut axis (determined by the two flexible joints) is critical and is inducing large variations in the dynamics from DAC voltage u to encoder measured displacement d_e. If encoders are to be used when fixed on the struts, it is therefore very important to properly align the APA and the flexible joints when mounting the struts.

In the next section, the struts are re-assembled with a "positioning pin" to better align the APA with the flexible joints. With a better alignment, the amplitude of the spurious resonances are expected to decrease as was shown in Figure 4.4a.

[1] Heidenhain MT25, specified accuracy of $\pm 0.5\,\mu m$

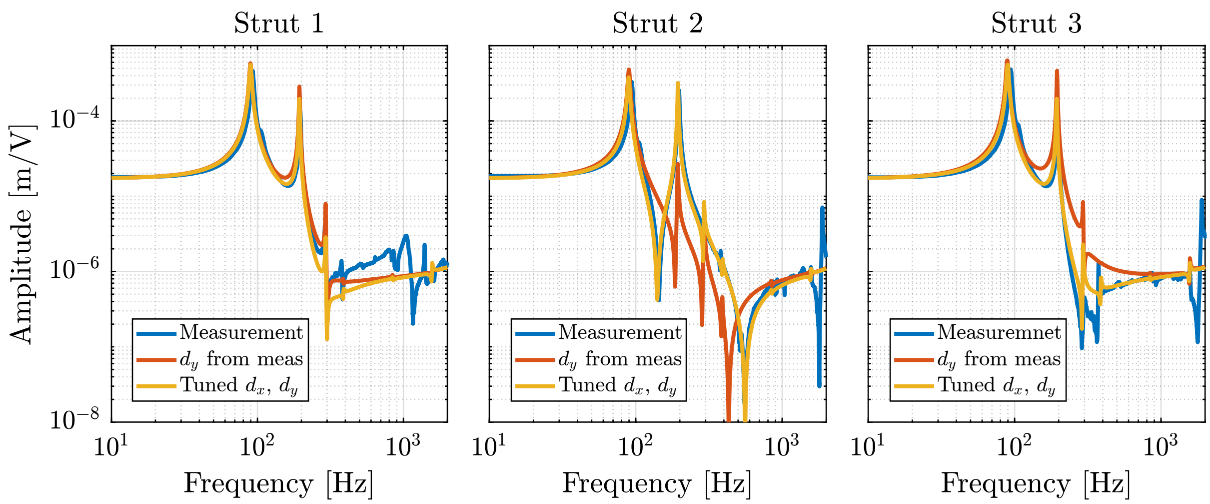

Figure 4.5: Comparison of the frequency response functions from DAC voltage u to measured displacement d_e by the encoders for three struts. The y misalignment between the APA and the flexible joints have been estimated

4.4 Comparison of all the (re-aligned) Struts

Should this be included here?

The struts are re-aligned and measured using the same test bench.

4.4.1 Measured misalignment of the APA and flexible joints

The misalignment between the APA and the flexible joints are measured.

The results are defined below and summarized in Table 4.2.

Table 4.2: Measured misalignment of the struts (`R` means "red" side, and `B` means "black side") in [mm]

Strut	R Top	B Top	R Bot	B Bot
1	-0.54	-0.5	-0.5	-0.52
2	-0.44	-0.55	-0.49	-0.49
3	-0.48	-0.5	-0.5	-0.46
4	-0.45	-0.51	-0.51	-0.45
5	-0.5	-0.5	-0.5	-0.5
6	-0.5	-0.49	-0.43	-0.54

Also, the sum of the measured distances on each side should be 1mm (equal to the thickness difference between the flexible joint and the APA). This is verified in Table 4.3.

The differences of the measured distances on each side corresponds to the misalignment on that same side (Table 4.4).

Table 4.3: Measured thickness difference between the flexible joints and the APA in [mm]

APA	Top	Bot
1	-1.04	-1.02
2	-0.99	-0.98
4	-0.98	-0.96
5	-0.96	-0.96
6	-1.0	-1.0
8	-0.99	-0.97

Table 4.4: Measured thickness difference between the flexible joints and the APA in [mm]

APA	Top	Bot
1	-0.02	0.01
2	0.055	0.0
4	0.01	-0.02
5	0.03	-0.03
6	0.0	0.0
8	-0.005	0.055

Important

After using the alignment pins, the misalignment of the APA and flexible joints are much smaller ($< 50\,\mu m$ for all the struts).

4.4.2 FRF Identification - Setup

The excitation signal is a low pass filtered white noise. Both the encoder and the force sensor voltage are measured.

Here are the leg numbers that have been measured. We get the frequency vector that will be the same for all the frequency domain analysis.

4.4.3 FRF Identification - Encoder

In this section, the dynamics from u to d_e (encoder) is identified.

Then, the transfer function from the DAC output voltage u to the measured displacement by the encoder d_e is computed: The obtained transfer functions are shown in Figure 4.6.

Important

Even though the struts are much better aligned, we still observe high variability between the struts for the transfer function from u to d_e.

figs/struts_align_frf_dvf_plant_tf.pdf

Figure 4.6: Estimated FRF for the DVF plant (transfer function from u to the encoder d_e)

4.4.4 Conclusion

Important

Having the struts well aligned does not change significantly the obtained dynamics.

The measured FRF are now saved for further use.

4.5 Effect of flexible joint's characteristics

As the struts are composed of one APA and two flexible joints, it is obvious that the flexible joint characteristics will change the dynamic behavior of the struts.

Using the Simscape model, the effect of the flexible joint's characteristics on the dynamics as measured on the test bench are studied:

- Section 4.5.1: the effects of a change of bending stiffness is studied
- Section 4.5.2: the effects of a change of axial stiffness is studied
- Section 4.5.3: the effects of a change of bending damping is studied

The studied dynamics is between u and the encoder displacement d_e.

4.5.1 Effect of bending stiffness of the flexible joints

Let's initialize an APA which is a little bit misaligned. The bending stiffnesses for which the dynamics is identified are defined below. Then the identification is performed for all the values of the bending stiffnesses. The obtained dynamics from DAC voltage to encoder measurements are compared in Figure 4.7.

Important

The bending stiffness of the joints has little impact on the transfer function from u to d_e.

figs/effect_enc_bending_stiff.pdf

Figure 4.7: Dynamics from DAC output to encoder for several bending stiffnesses

4.5.2 Effect of axial stiffness of the flexible joints

The axial stiffnesses for which the dynamics is identified are defined below. Then the identification is performed for all the values of the bending stiffnesses. The obtained dynamics from DAC voltage to encoder measurements are compared in Figure 4.8.

figs/effect_enc_axial_stiff.pdf

Figure 4.8: Dynamics from DAC output to encoder for several axial stiffnesses

Important

The axial stiffness of the flexible joint has a large impact on the frequency of the complex conjugate zero. Using the measured FRF on the test-bench, if is therefore possible to estimate the axial stiffness of the flexible joints from the location of the zero.
This method gives nice match between the measured FRF and the one extracted from the simscape model, however it could give not so accurate values of the joint's axial stiffness as other factors are also influencing the location of the zero.
Using this method, an axial stiffness of $70 N/\mu m$ is found to give good results (and is reasonable based on the finite element models).

4.5.3 Effect of bending damping

Now let's study the effect of the bending damping of the flexible joints.

The tested bending damping are defined below: Then the identification is performed for all the values of the bending damping. The results are shown in Figure 4.9.

figs/effect_enc_bending_damp.pdf

Figure 4.9: Dynamics from DAC output to encoder for several bending damping

5 Conclusion